韓國水資源學會誌 論文
第29卷 第1號·1996年 2月
pp. 249~263

고정케이블에 작용하는 Icing 하중: I. 실험

Icing Loads on Fixed Cables : I. Laboratory Experiments

윤 병 만* · Ettema, R.**
Yoon, B. • Ettema, R.

Abstract

Presented herein are the results of a laboratory study on structural loads (icing weight and wind loads) associated with icing formation on rigidly fixed, circular power-transmission cables and cylinders. The experiments were carried out using movable wind tunnel under two different conditions: refrigerated and non-refrigerated conditions. Temporal evolution of icing loads were determined in the refrigerated laboratory and wind loads for icings at several stages of icing formation were measured in the non-refrigerated laboratory.

요 지

본 논문에서는 고정된 전선과 원형 실린더에 부착되는 icing으로 인해 발생되는 하중(icing의 무게 및 풍하중)에 관한 실험을 수행하고 그 결과를 수록하였다. 실험은 이동 가능한 풍동을 이용하여 냉동실 실험과 실온 실험으로 구분하여 실시하였다. 냉동실 실험에서는 icing으로 인한 하중의 시간적 변화를 측정하였으며, 실온 실험에서는 특수 제작한 icing 모형을 이용하여 풍속 변화에 따른 풍하중 변동을 측정하였다.

1. Introduction

Icings accumulated from airborne water droplets, freezing rain and wet snow pose major hazards for land-based structures, such as electric-power transmission towers and the cables they support. Occasionally, towers are loaded to the extent that they collapse. Some interesting descriptions of tower collapse are reported by Kuroiwa (1965), Shira(1978), and Fikke et al. (1983). The failures of such structures are attributable not only to icing weight, but often to icing-induced (or aggravated) wind loads. A

* 명지대학교 공과대학 토목공학과 조교수
** Iowa Institute of Hydraulic Research and College of Engineering, The University of Iowa, USA

particularly good case study description of ice-aggravated wind loading is given by Govoni and Ackley (1986).

The preponderance of icing literature deals with icing weight, comparatively little having been published on wind loads. One study, for example, that by McComber and Bouchard (1986), entailed the use of a numerical model to determine aerodynamic drag and lift coefficients. For a given icing shape, it gave values of drag and lift coefficients, but the method has not been rigorously tested. Koutselos and Tunstall(1986) provide a limited number of results from experimental studies of icings on circular cylinders and cables, but their results do not elucidate the temporal variation of wind load as icings form, and no attempt was made to characterize icing wind loads. Other studies, such as those by Jones and Govoni (1990), McComber et al. (1983), Krishnasamy (1983), and Govoni and Ackley (1983) provide useful data indicating the strong dependence of icing wind load on parameters as icing shape and surface texture, but their data are neither adequately detailed nor extensive to enable load relationships to be developed including those parameters.

For general design purposes, more information is required to relate icing loads to size of collector element being iced, icing shape and density, etc. There is, in particular, a need to obtain more accurate information about wind loads. The present study attempts to contribute toward meeting this need. Load data were obtained from experiments in a refrigerated laboratory, and analyzed to correlate icing loads with cylinder or cable diameter. Also examined was the time evolution of the icing loads (weight, lift and drag) as icings form.

2. Wind Tunnel

The experiments were conducted using an icing wind tunnel, whose layout and principal dimensions are shown in Fig. la. The tunnel has a square, 0.6m×0.6m, test section which is 2.5-meter-long and is enclosed by plexiglass. The tunnel comprises four detachable units, and is readily movable, so that it can be operated either in a refrigerated laboratory, outdoors under frigid weather conditions, or in a non-refrigerated laboratory.

Speeds in the range of 0 to about 30 m/s are attainable by means of a vane-axial fan operated at the upstream end of the wind tunnel. Boundary layers develop along the four walls of the test section, becoming approximately 40- and 50-millimeters -thick at the upstream and downstream ends of the test section, respectively. Thus the net width of uniform flow through the test section is about 500 mm. The tunnel is equipped with two spray nozzles positioned just downstream of the flow-conditioner section (see Fig. 1a). They enable injection of water droplets of approximately controlled size and amount. The spray nozzles and tubing for water and air supply system were enclosed in an airfoil in order to minimize the flow disturbance through the tunnel. Other design criteria and performance of the tunnel are summarized by Jovic et al. (1986).

3. Experiments

The program of experiments was carried out in two parts. The first part entailed experiments with the icing wind tunnel placed in the refrigerated laboratory. In this part, the time evolution of icing loads was monitored. The second part entailed experiments with the wind tunnel oper-

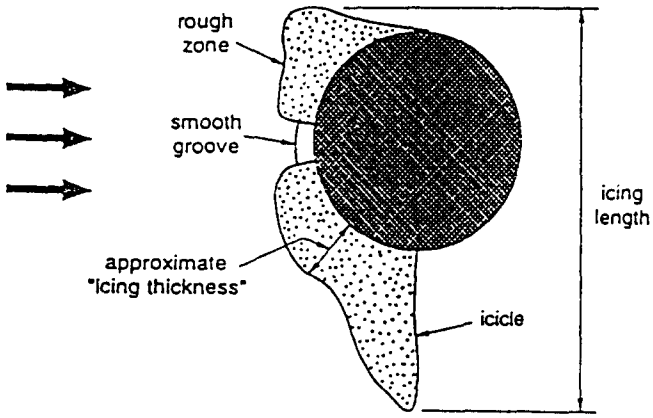

(a) Glaze Icing

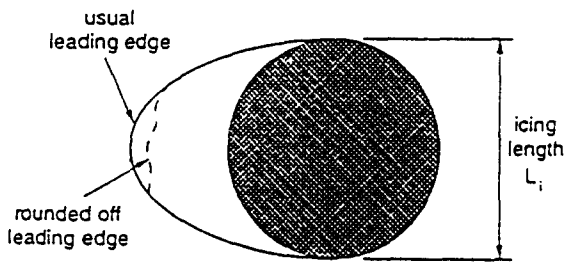

(b) Rime Icing

Fig. 1. Definition of Icing Length

ated to produce a range of wind speeds in a non-refrigerated laboratory using modeled forms replicating icings grown in the refrigerated laboratory.

3.1 Experimental Set-Up

Five cylinders, or collectors, were used in this study. Two were 25 and 56-millimeter-diameter aluminum tubes. The remaining three were electric-power transmission cables, 10, 17, 26 mm in diameter. Each of the five collectors was supported from the free-standing instrument frame as shown in Fig. 1b. The frame isolated the collectors and the instrumentation from tunnel vibrations. The collectors were aligned horizontally across the wind tunnel and normal to the wind direction. Each was supported at one end by a load cell, and at the other end by a low-friction bearing. A 75-millimeter-diameter hole was made on each side wall of the wind tunnel to maintain clearance between the wind tunnel wall and the collectors. The end of each collector was fitted with an adapter to facilitate easy exchange of collectors under low-temperature conditions. The bearing end also permitted thermally-induced longitudinal deformation of the collectors.

A multi-component load cell was used to measure two orthogonal force components acting perpendicular to the axial direction. Outputs from the load cell were recorded and ana-

lyzed on-line using a computer.

3.2 Experimental Procedures: Refrigerated Conditions

After a series of preliminary experiments at various windspeeds, it was decided that the refrigerated experiments should be carried out with an air speed of 10 m/sec. This wind speed allowed a uniform icing to grow within a reasonable time period. It was considered that this wind speed would be suitable for producing the different icing types, in accordance with variations of air temperature and moisture-flow rate. Wind speed was checked using a pitot tube, and the fluctuation was within 5 percent during the experiment.

An additional set of preliminary experiments was performed to determine a moisture -flow rate that would produce icings that varied from glaze to rime by adjusting the temperature. It was found that a moisture-flow rate of 3.6 liters per hour satisfied that need. At higher temperatures (-5℃ and -10℃), glaze icing formed. At the lower temperature (-15℃), rime icings formed.

A period of 30 minutes was selected as the duration for each experiment. This period was selected as being reasonabe representative of icing events, and so that icicles would not significantly block the test section.

It should be noted that icing weight could not be determined directly during tunnel operation, because the load cell measured only a net vertical force, which consisted of icing weight plus wind lift. To determine icing weight during accretion, the total period of data acquisition was divided into three 12-minute periods. During each period, the spray system was operated continuously for 10 minutes, while the data was logged for 12 minutes to include the wind loading during start-up and shutdown periods. This procedure enabled acquisition of additional information on icing weight and wind lift after 10 and 20 minutes of icing accretion.

The experiments were carried out with the icing wind tunnel placed in a refrigerated laboratory where air temperature could be controlled. To ensure that ambient moisture content of the air in the laboratory remained more-or-less constant, a wire-mesh grid was placed a short distance downstream of the wind tunnel to catch and freeze moisture exhausted from it. The wire-mesh grid can be seen in Fig. 1b.

The primary objective of these experiments was to collect a fairly extensive set of load data under controlled experimental conditions (air temperature, wind speed, moisture-flow rate, etc.) so that quantitative comparisons could be made to ascertain the influence of air temperature, and cylinder or cable diameter on the weight and wind loads incurred with icing formation.

3.3 Experimental Procedure : Non-refrigerated Conditions

For the non-refrigerated experiments, seven icing forms were made. The forms were of icings accreted on the 56-millimeter-diameter, smooth aluminum pipe, and for a moisture-flow rate of 3.6 liters per hour. Three forms were of rime icings at three stages of formation (10, 20 and 30 minutes). They were made with sheet metal with sandgrain roughness finish; their surface roughness was the same as for the actual icings. The remaining four icing forms were replications of glaze icings made, with some difficulty, by means of a special molding technique. The detailed procedure for making molds from fiber-glass resin is described by Yoon (1991). Three forms correspond to a glaze icing, created at -10℃, after 10, 20 and 30 minutes of icing. The remaining form repli-

cated a glaze icing formed after 30 minutes at −5℃.

For each icing form, wind drag and lift were measured at various wind speeds (8, 12, 16 and 20 m/sec) to determine how drag and lift coefficients vary with Reynolds number. The wind loads were measured using the same experimental set-up used in the refrigerated wind tunnel experiments.

4. Results

4.1 Observations and Measurements

For the ranges of ambient air temperature and moisture-flow rate considered in this study, it was possible to produce icings which varied from glaze to rime. Rime icings were observed at temperatures of −15℃ or less in the test set up. They formed more-or-less symmetrical shapes, similar to those observed and reported by Lozowski et al. (1983). Glaze icings were observed at −5℃ and −10℃. They were markedly unsymmetric in form with icings observed and reported by others (e.g., Lozowski et al., 1983); in the present study, icicle formation can be attributed to the lower air speed. In contrast to the rime icings, glaze icings showed limited growth at the stagnation line, as illustrated in a comparison of Figs. 2 and 3.

Figs. 2 and 3 illustrate the principal features of glaze and rime icing formation, respectively, produced when the icing wind tunnel was operated in the refrigerated laboratory with a moisture-flow rate of 3.6 liters per hour and air temperatures ranging from −5℃ to −10℃. As evident in Figs. 2 and 3, the size and geometries of glaze and rime icings are affected by the bare cylinder or cable diameter, D.

Measured icing loads were converted using the following set of equations, and in accordance with the foregoing conversion procedure, to forces per unit span length. Icing weight per unit length, $\overline{W}$, was evaluated herein as

$$\overline{W}=\frac{W}{pB} \tag{1}$$

Lift per unit length, $\overline{F}_L$, was evaluated as

$$\overline{F}_L=\frac{F_L}{pB} \tag{2}$$

Drag per unit length, $\overline{F}_D$, was assessed as

$$\overline{F}_D=[F_D-F_0(1-p)]/pB \tag{3}$$

in which W, F_L and F_D = measured weight, lift and drag, respectively; F_0 = initial cylinder/cable drag without icing; and p = ratio of effective span (B_e) to width of the wind tunnel's test section, B. For rime icings, effective span is defined herein as the span-wise length of icing accretion if the icing had accreted uniformly. Fig. 4a illustrates this definition. For glaze icings, the span-wise length was selected as the effective span, as shown in Fig. 4b, for which icings were reasonably uniform in length.

4.2 Time Evolution of Weight and Wind Loads

Figs. 5(a) and (b) show two typical time histories of vertical force component (weight plus lift) measured during icing of the 10-millimeter-diameter cable. One time history (Fig. 5(a)) is associated with glaze-icing formation. The other (Fig. 5(b)) is associated with rime icing. There are three peak values in loading curves which denote icing weight at 10, 20 and 30 minutes, respectively, for those experiments.

For glaze icings, icing weight increased nonlinearly with time due to the significant in-

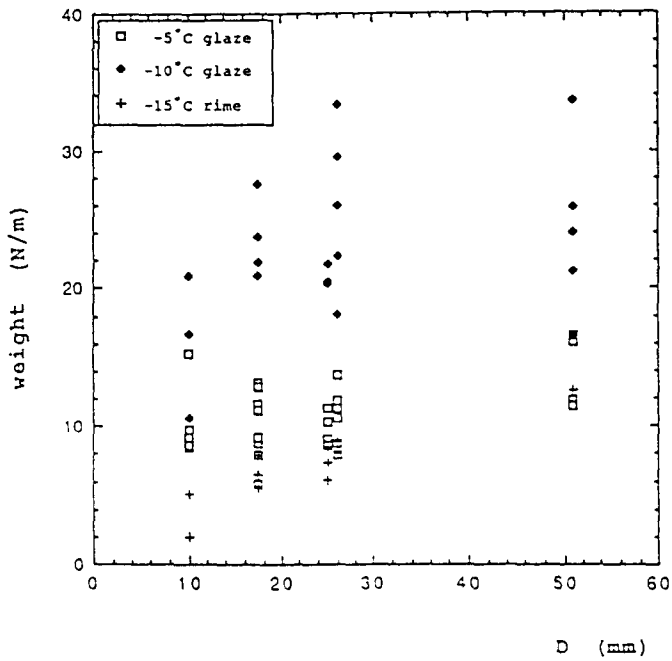

Fig. 2. Icing Weight versus Collector Diameter

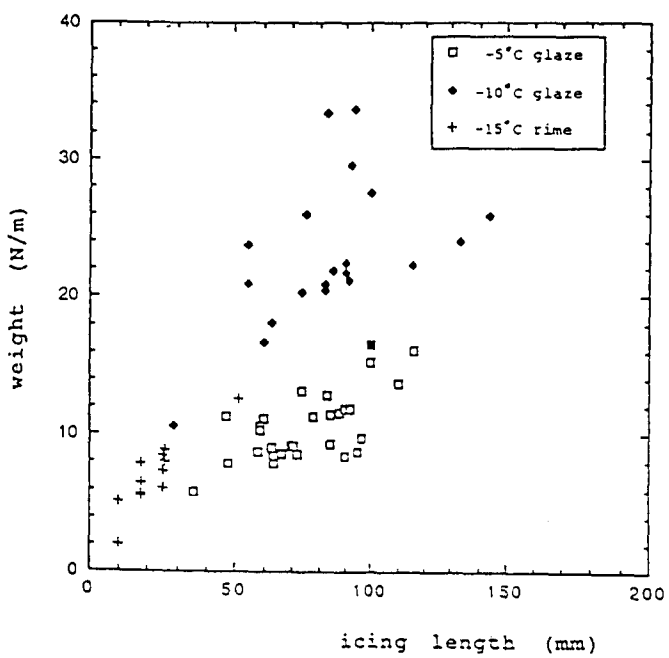

Fig. 3. Icing Weight versus Icing Length

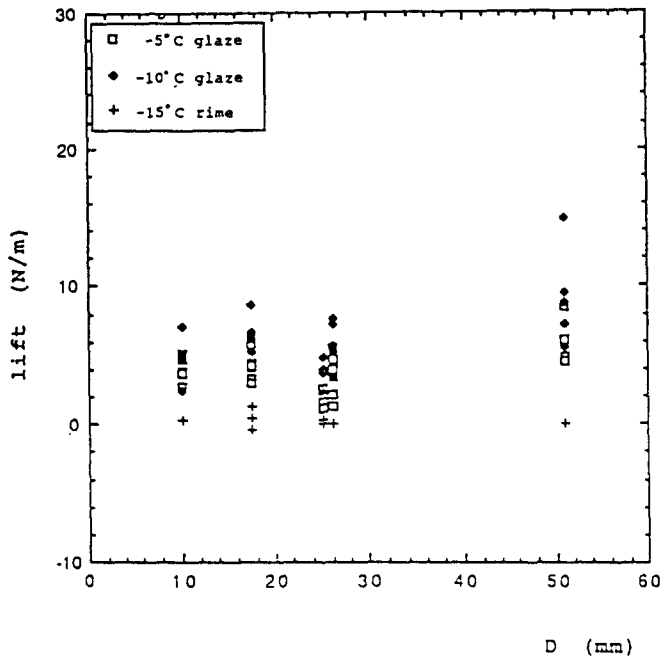

Fig. 4. Lift versus Collector Diameter

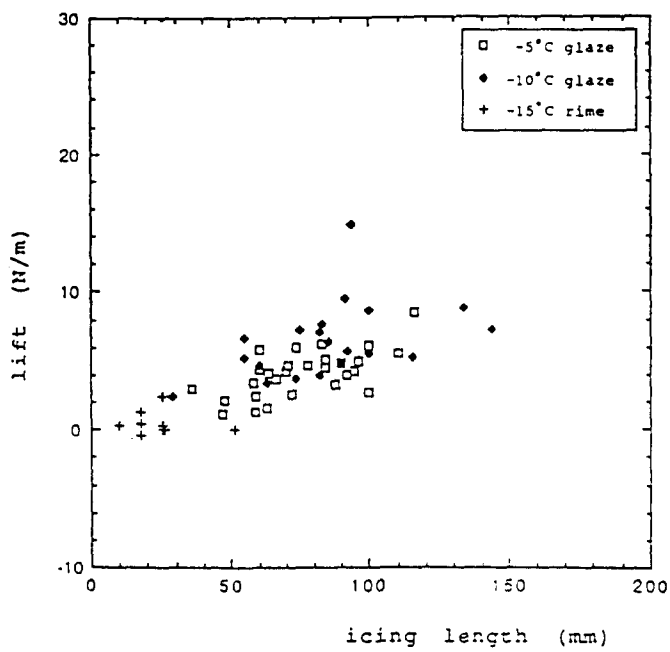

Fig. 5. Lift versus Icing Length

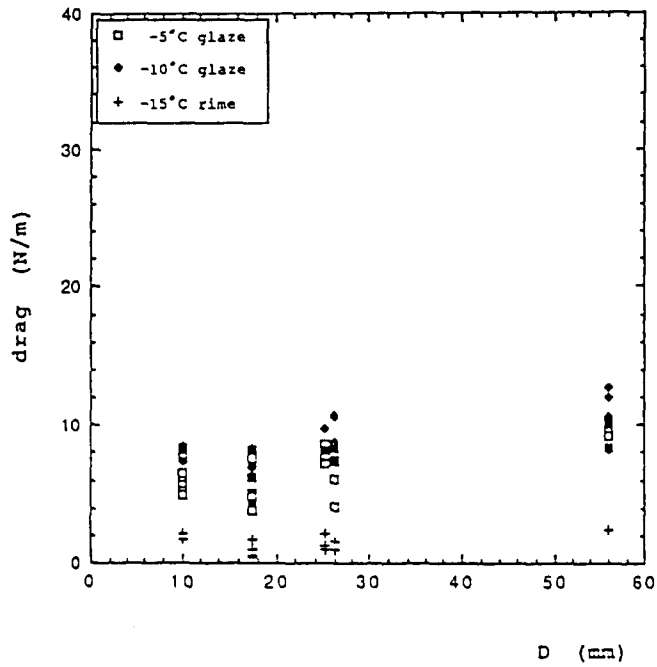

Fig. 6. Drag versus Collector Diameter

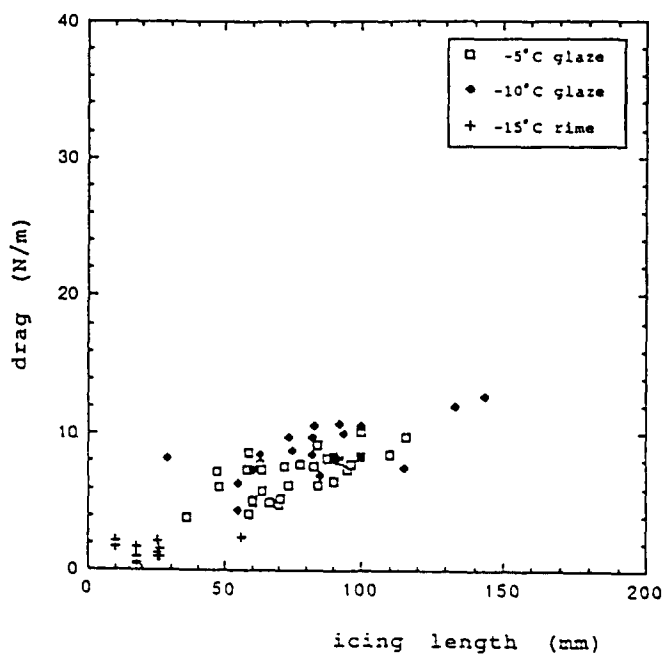

Fig. 7. Drag versus Icing Length

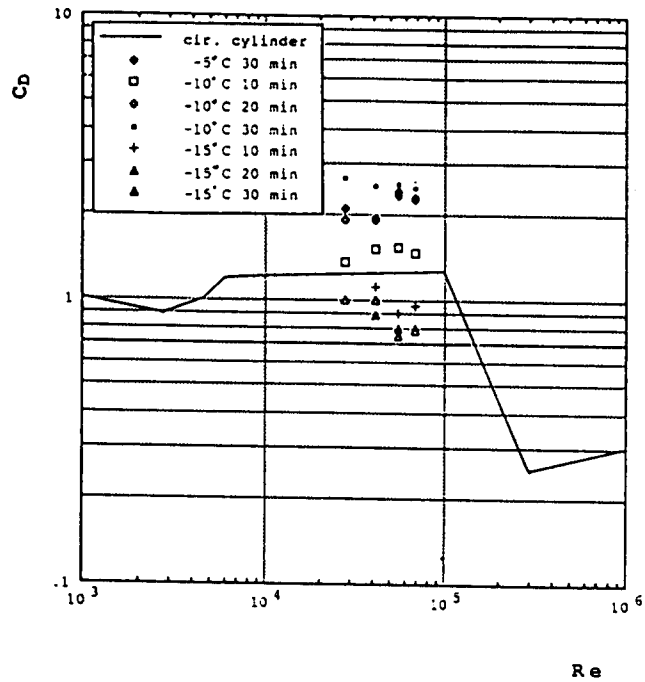

Fig. 8. Drag Coefficient, C_D, in terms of Re, with D Used as Characteristic Length

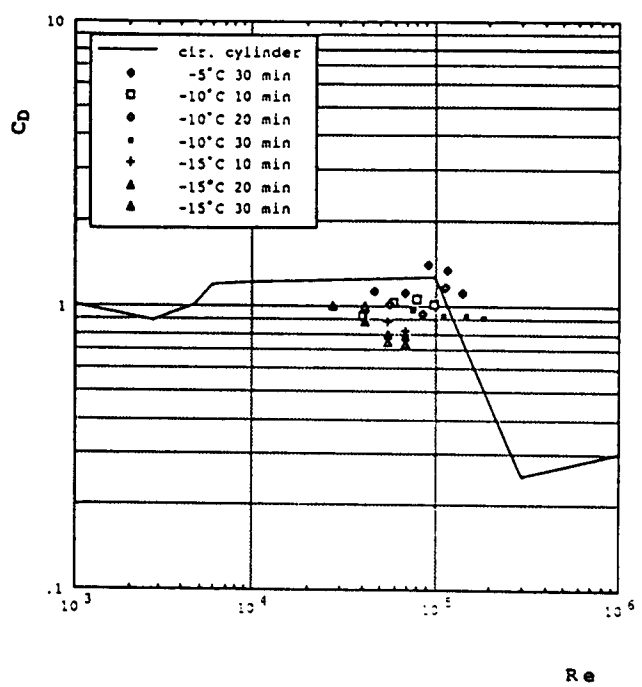

Fig. 9. Drag Coefficient, C_D, in terms of Re, with L_i Used as Characteristic Length

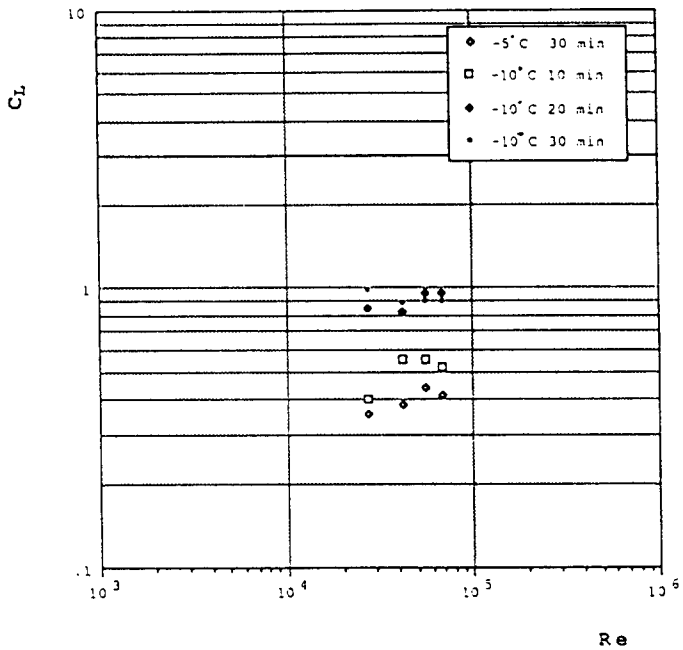

Fig. 10. Drag Coefficient, C_D, in terms of Re, with D Used as Characteristic Length

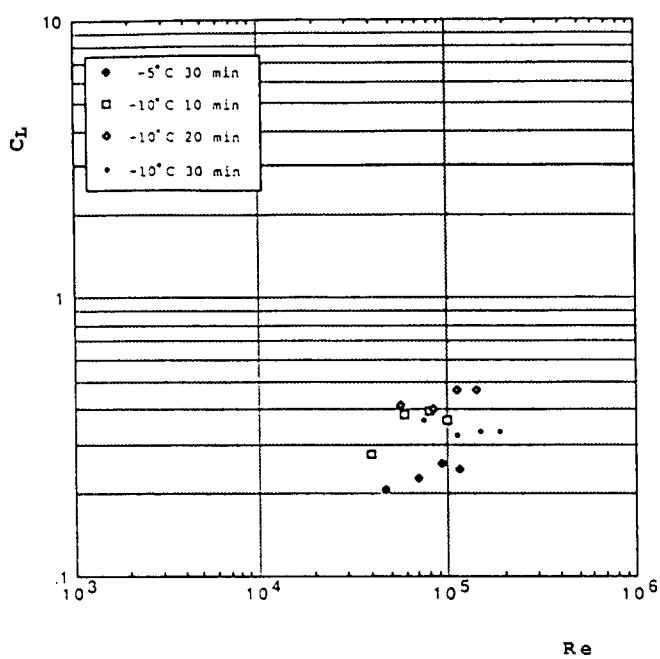

Fig. 11. Drag Coefficient, C_D, in terms of Re, with L_i Used as Characteristic Length

crease in frontal area of collector that resulted with icicle formation, as shown in Fig. 6a; i. e.,

$$\overline{W} \propto t^m \tag{4}$$

Makkonen (1984) showed that ice load is nonlinear with time during wet growth, but gave no value for indices m. Diem (1956) stated a relation that ice load is proportional to $t^{1.4}$. McComber (1983) showed that accretion rate increased with time. Based on the time-records of icing weight in this study, the exponent, m, varied approximately between 1.0 and 1.3.

For rime icings, on the other hand, icing weight essentially increased linearly, as shown in Fig. 5(b); i.e., m = 1. This finding is explainable in terms of the projected frontal area, collection efficiency and freezing fraction, all of which remained practically constant during rime-icing formation.

The magnitude of lift force can be assessed from the sharp jump, after 1 minute periods of icing, in the loading curve, as shown in Fig. 5a. For glaze icings, lift increased nonlinearly (the exponent was found to vary approximately from 1.1 to 2.3) with time as icicles grow; at least for the experimental conditions and period used in the present study. It is well known that aerodynamic lift acts perpendicularly to the relative velocity of a bluff body. In this case, as the motion of the test span was prevented, the lift force acts parallel to the weight. Also, in this case, lift reduces the net vertical load, or opposes the icing weight. This result is at variance with the observations of McComber et al. (1983) and a few other studies which suggest that lift force increases the overall vertical load. Icing weight, though, is much greater in magnitude than lift. For example, Fig. 5(a) shows that lift is only about 20 percent of weight.

For rime icings, the net vertical force did not change when air flow ceased, as shown in Fig. 5 (b). Consequently, insofar that the rime-icings were axisymmetric in form, lift was negligible for rime icings during the entire period of experiment. McComber et al. (1983) likewise found that significant aerodynamic lift is not generated by a dry rime icing shape.

Fig. 6(a) and (b) show selected time histories of wind drag measured from the 10-millimeter-diameter cable undergoing glaze- and rime-icing formation. The time histories are representative of those obtained during the experiments. The initial rise in drag is attributable to increasing wind speed as the wind tunnel was started. It appears from Figs. 6(a) and (b) that drag decreases during the initial stage of icing accretion. Since little icing has formed at this stage of development, the drag reduction is probably due to the smoothing of the cable as ice fills the stranding. After this initial reduction, wind drag changed slowly with time. For glaze icings, drag increased gradually immediately after the initial sharp reduction, as shown in Fig. 6(a). For rime icings, however, drag decreased gradually, as shown in Fig. 6(b), because rime-icing shape remained symmetric and became more streamlined with time.

4.3 Variation of Loads with Cylinder/Cable Diameter

Fig. 7 presents values of icing weight, $\overline{W}$, after 30 minutes of icing accretion, plotted versus cable or cylinder diameter, D. Air temperature is a third parameter in Fig. 7. For rime icings (data points shown as "+" in Fig. 7), icing weight varied more or less linearly with D. However, it is very difficult to determine an equally simple relation between icing weight and D for the glaze icings.

Fig. 8 presents values of lift per unit length, after 30-minutes accretion, versus cylinder or

cable diameter, with air temperature as a third parameter. Lift was generally small compared with weight and, as noted, it acted in the opposite direction to weight. The influences of freezing fraction and air temperature on lift are smaller than on icing weight. Fig. 8 also shows that lift forces exerted against rime icings are negligible, in keeping with their virtually symmetric cross-sectional shapes. As seen in Fig. 8, there is no relationship between cable diameter and lift forces.

Fig. 9 presents values of drag force exerted against icing formed after 30 minutes of formation. The values are plotted versus cylinder or cable diameter with air temperature as a third parameter. Drag force exerted against glaze icings, most of which were formed at -5℃ and -10℃, is greater than that exerted against rime icings formed at -15℃. As anticipated, this result demonstrates that icicles significantly increase drag. For icings formed at all temperatures, drag force increased only gradually with increasing cylinder or cable diameter. For glaze icings formed at -5℃ and -10℃, however, drag exerted against the smallest cable (D = 10 mm) was, on average, about same as that exerted against icings formed on the 17.5 mm cable. At these two test conditions, icicle formation completely dominated icing form, size, and therefore drag. Generally, the glaze-icing data are scattered; a result which can be interpreted to mean that drag against glaze icings, like glaze-icing weight, is not markedly dependent on the cylinder or cable diameter.

4.4 Influences of Wind Speed on Icing Wind Loads

Icings may form during wind of a certain speed, but once formed, and no longer growing, they may generate wind loads that vary with wind speed. The resulting drag and lift forces then differ from those occurring during icing formation. The present study set out to determine how drag and lift forces exerted against performed icings vary with wind speed. More precisely, it set out to determine representative drag and lift coefficients associated with typical icing forms, and to investigate how those force coefficients vary with Reynolds number (Re) of flow around icings.

Drag coefficient, C_D, is shown in Fig. 10, in terms of Reynolds number, Re. For two-dimensional body, C_D and Re are defined respectively as

$$C_D=\frac{\bar{F}_D}{\frac{1}{2}\rho_a V_0^2 D} \tag{5}$$

and

$$Re=V_0 D \tag{6}$$

in which υ_a = kinematic viscosity of air.

For glaze icings, as is evident in Fig. 10, values of C_D

are higher than those of the smooth circular cylinder, for which C_D = 1.2, and increase with stage of icing development; at least for the conditions considered in the present study. For the rime icings, however, values of C_D are less than those of the smooth circular cylinder. Moreover, they gradually decrease with stage of icing development, at least for the conditions considered in this study. However, the differences in C_D values between different stages of rime-icing development are not as clear as for glaze icings.

For a given glaze-icing form, C_D is expected to be constant and of a higher magnitude than the circular cylinder for values of Re within 5 × 10^3 to 10^5, since glaze icings essentially behave like bluff bodies in air flow. This expectation is verified in Fig. 10, as values of C_D for ic-

ings formed at −10℃ after 10, 20 and 30 minutes remain virtually constant at 1.5, 2.1 and 2.5, respectively. These values show that C_D increases with stage of glaze-icing formation. For the glaze icing formed after 30 minutes at −5℃, C_D = 2.1. The slight variations in values of C_D determined for icings formed at a given air temperature and period of formation are attributable to slight changes in local flow characteristics due to icicles.

The variation of C_D with Re for rime icings is different from that for glaze icings. Since rime-icing formation streamlined the leading perimeter of the circular cylinders, C_D was reduced from the value for a circular cylinder. Fig. 10 also shows that values of C_D associated with rime icings decrease with Re. This trend probably occurred because the data of this Re range (between 2×10^4 and 7×10^4) are in what is commonly known as the drag-crisis zone, for which the boundary layer around a body changes abruptly from laminar to turbulent flow, with a consequent marked thinning of the wake. Consequently, the values of C_D determined for the rime icings decrease with Re over the Re range considered in this study. Rime icings have smaller values of C_D and encounter drag crisis at lower values of Re than do circular cylinders because of their streamlined leading edge and small roughness on the surface.

As lift forces exerted against rime-icing forms were found to be negligible, they were measured only for the glaze-icing models. Fig. 11 presents values of C_L for four glaze-icing forms in terms of Re. Note that C_L is calculated herein as

$$C_L = \frac{\bar{F}_L}{\frac{1}{2}\rho_a V_0^2 D} \tag{7}$$

Fig. 11 indicates that values of C_L range from about 0.3 to about 1.0, and shows clearly the difference between the values of lift exerted against each icing form used in the experiment.

5. Conclusions and Recommendations

The experimental results obtained from this laboratory study reveal that icing weight generally is the predominant icing load for the temperature range considered in this study. However, for glaze icings, increased drag can be of comparable magnitude to net vertical force, especially for slender structural elements and cables. Therefore, it is important that drag as well as icing weight be taken into account. In practical terms, lift is negligible for rime icings. Even for glaze icings, lift is small (less than 20%) compared to icing weight. Although lift seems not to be so important in magnitude, its effect cannot be neglected entirely because it may initiate catastrophic vibrations, in the form of a galloping conductors or oscillating guy wires.

The time evolution of icing weight for glaze icings was proportional to $t^{1.0}$ to $t^{1.3}$ for the data collected during this study. Rime icing weight, however, increased essentially linearly with time. The rime icings did not produce lift forces, and the drag forces associated decreased linearly with time due to their streamlined, symmetric shape. Glaze icings produce lift forces which increased nonlinearly with time, lift evolves at a rate proportional to $t^{1.1}$ to $t^{2.3}$. Drag associated with glaze icings increased linearly with time.

For a given icing form, the value of C_D appeared to be constant within the Reynolds number range of 5×10^3 to 10^5. The values of C_D for glaze icings formed at −10℃ after 10, 20, 30 minutes are 1.5, 2.1 and 2.5, respectively. For the glaze icing formed at −15℃ after 30 minutes, C_D is 2.1. The values of C_D for rime icing

forms are smaller than that of smooth circular cylinder and decrease with Reynolds number within the Re range (2×10^4 to 7×10^4) considered in this study. Lift coefficient, C_L, for glaze icings ranges from about 0.3 to about 1.0.

For glaze icings, the icing loads were not simply dependent on D, because development of icicles substantially increased cylinder or cable frontal area. It is, therefore, recommended to investigate into determination of proper length scale which represents the characteristics of icing geometry.

Acknowledgment

This study was supported by funds provided by the U. S. National Science Foundation under grant No. CES-861185, and by funds provided by the Electric Power Research in Iowa (EPRIa) program, which is supported by Iowa's investor-owned electric-power utilities.

References

Diem, M. (1956). "Ice loads on high voltage conductors in the mountains." Arch. *Meteor. Geophys. Bioklim.*, Vol. B7, pp. 84-95 (in German).

Fikke, S.M., Schjetne, K., and Evensen, B.D. (1983). "Iceload measurements and design practice." *Proceedings of First International Workshop on Atmospheric Icings of Structures*, CRREL Special Report 83-17, U.S. Army Cold Regions Research and Engineering Laboratory.

Govoni, J.W., and Ackley, S.F. (1983). "Field measurements of combined icing and wind loads on wires." *Proceedings of first International Workshop on Atmospheric Icing of Structures*, CRREL Special Report 83-17, U.S. Army Cold Regions Research and Engineering Laboratory.

Govoni, J.W., and Ackley, S.F. (1986). "Icing and wind loading on a simulated power line." *The Northern Engineer*, Vol. 18, No. 1, pp. 23-27.

Jones, K.F., and Govoni, J.W. (1990). "Aerodynamic properties of natural rime ice samples." *Proceedings of Fifth International Workshop on Atmospheric Icing of Structures.*

Jovic, S., Ettema, R., and Kennedy, J.F. (1986). "Performance requirements, design and operation of Iowa icing wind tunnel." *Proceedings of Third International Workshop on Atmospheric Icing of Structures.*

Koutselos, L.T., and Tunstall, M.J. (1986). "Collection and reproduction of natural ice shapes on overhead line conductors and measurement of their aerodynamic characteristics." *Proceedings of Third International Workshop on Atmospheric Icing of Structures.*

Krishnasamy, S.G. (1983). "Measurement of ice accretion on overhead transmission line conductors." *Proceedings of First International Workshop on Atmospheric Icing of Structures*, CRREL Special Report 83-17, U.S. Army Cold Regions Research and Engineering Laboratory.

Kuroiwa, D. (1965). "Icing and snow accretion on elective wires." *CRREL Report 123*, U.S. Army Cold Regions Research and Engineering Laboratory.

Lozowski, E.P., Stallbrass, J.R., and Hearty, P.F. (1983). "The icing of an unheated, nonrotating cylinder: Part II. Icing windtunnel experiments." *Journal of Climate and Applied Meteorology*, Vol. 22, pp. 2062-2074.

Makkonen, L. (1984). "Modeling of ice accretion on wires." *Journal of Climate and Applied Meteorology*, Vol. 23, pp. 929-939.

McComber, P. (1983). "Numerical simulation of ice accretion on cables." *Proceedings of First International Workshop on Atmospheric Icing of Structures*, CRREL Special Report 83-17, U.S. Army Cold Regions Research and Engineering Laboratory.

McComber, P., Morin, G., Martin, R., and Vo Van, L. (1983). "Estimation of combined ice and wind load on overhead transmission lines." *Cold*

Regions Science and Technology, Vol. 6, pp. 195–206.

McComber, P., and Bouchard, G. (1986). "The numerical calculation of the wind force coefficients on two dimensional iced structures." *Proceedings of Third International Workshop on Atmospheric Icing of Structures.*

Shira, D.L. (1978). "Hydroelectric power plant siting in glacial areas of Alaska." *Proceedings of ASCE Specialty Conference on Cold Environmental Technology*, Anchorage, AL, USA.

Yoon, B. (1991). "A study of atmospheric-icing formation and forces," Ph.D. thesis, The University of Iowa.

〈접수 : 1995년 10월 12일〉